APL Photonics

Optical clearing and shielding with fan-shaped vortex beams (F)

Haiping Wang, Liqin Tang (iD), Jina Ma, Huiwen Hao, Xiuyan Zheng, Daohong Song, Yi Hu, Yigang Li, and Zhigang Chen (iD)

COLLECTIONS

(F) This paper was selected as Featured

View Online   Export Citation   CrossMark

AIP Publishing

Optical clearing and shielding with fan-shaped vortex beams ⒻⓈⒸⒾ

Haiping Wang,[1] Liqin Tang,[1,2,a] ⒾⒹ Jina Ma,[1] Huiwen Hao,[1] Xiuyan Zheng,[1] Daohong Song,[1,2] Yi Hu,[1,2] Yigang Li,[1,2] and Zhigang Chen[1,2,3,b] ⒾⒹ

AFFILIATIONS

[1] The MOE Key Laboratory of Weak-Light Nonlinear Photonics, TEDA Applied Physics Institute and School of Physics, Nankai University, Tianjin 300457, China
[2] Collaborative Innovation Center of Extreme Optics, Shanxi University, Taiyuan, Shanxi 030006, People's Republic of China
[3] Department of Physics and Astronomy, San Francisco State University, San Francisco, California 94132, USA

a) tanya@nankai.edu.cn
b) zgchen@nankai.edu.cn

ABSTRACT

We propose and demonstrate a new method for creation of fan-shaped optical vortex beams by rational phase modulation and assembly based on a well-known conical vortex phase. Our design is different from the previously proposed method for generation of power-exponential vortex beams. Such unconventional vortex beams consist of multiple spiral beam filaments (as the fan blades), and their overall beam size and spiral angle can be readily controlled by adjusting the parameters. Experimentally, two examples of applications are illustrated with such fan-shaped vortex beams: one is optical clearing through densely scattering particle suspensions; the other is optical shielding and transporting a target particle from the suspensions by adding a donut pattern in the center (as the fan head). We envisage such specially designed fan beams may be used as a multifunctional tool for microfluidic and biological applications that involve the complex environment of the living bodies, especially for active isolation or separation of a trapped particle from fluid environments of high particle concentrations.

I. INTRODUCTION

Due to Ashkin's pioneering work,[1,2] optical tweezers have been widely used as a versatile tool in many areas such as biology and life science,[3–6] atom assembly,[7–9] and plasmonics.[10–12] In particular, as one of the powerful tools, optical tweezers empowered by specially shaped optical beams play an essential role in multidimensional optical trapping and particle transportations.[13–20] For example, a vortex beam can rotate a microparticle or a cluster of microparticles at ease, and a Bessel beam can be employed to trap different types of microparticles in three dimensions.[21,22] Even though optical tweezers can be used as a nontouching tool, in practical experiments, a trapped particle or cell is often perturbed by surrounding particles or impurities due to the Brownian motion in the fluid environment. As such, diluted samples with very low particle or cell concentrations are typically used.[23–26] Even so, the target particle is still susceptible to ambient perturbations with the passage of experimental time. To reduce such unwanted influence on the trapped particle, manual movement of the trap and/or the sample is often needed.

In recent years, in order to overcome the disturbance from ambient perturbation, various beam shaping techniques have been developed and implemented with an optical trapping system. For instance, self-accelerating airy beams have been used for optically mediated particle clearing,[27,28] donut-shaped Laguerre–Gaussian beams have been added to the optical tweezer setup as an optical shield to exclude contaminating particles, and optical bottle beams have also been used as a shield to protect trapped particles.[29,30] During the process of transporting a target object, specially designed holographic optical tweezers can automatically bypass the incoming particles in real-time without manual manipulation.[31,32] Most of these methods involve either complex manual manipulation or

user control as well as heavy calculations by the optical tweezers tool since they are based on passively eluding the impurities. Thus, it is desirable to have an optical tweezer tool with active clearing and transporting functions through densely scattering particle suspensions and related environments.

In this work, inspired by the fact that an electric fan can blow away the impurities in air, we design and demonstrate rotary fan-shaped optical vortex beams (FOVBs) that can be applied for active optical clearing and transportation of a trapped particle in liquids. Specifically, we first propose a new method for the generation of a spiral beam by judicious phase modulation based on conical (symmetric) vortex beams, with precise control of the size and angle of the spiral, which forms one blade of the FOVB. Our design is different from the previously proposed method for generation of power-exponential vortex beams.[33,34] Then, we "assemble" three such spiral beams into a fan-shaped vortex beam with an intensity pattern akin to three blades. More importantly, two examples of applications are illustrated with such FOVBs: First, an FOVB is used for optical clearing—the rotating fan blades "blow" away polystyrene particles in a target area in the colloidal suspension, thus actively keeping the area clean for a long time. Second, by adding a hollow beam in the center as the fan head, a target particle is trapped in the center and protected by the rotating fans since any intruding impurities are blown away even during the transportation of the target particle. Our design may presage an effective photonic tool for optical trapping and manipulation, especially when shielding and transporting of a trapped particle through fluid environments of high particle concentrations is unavoidable.

II. METHOD AND RESULTS

The orbital angular momentum (OAM) of an optical vortex beam can be transferred into the rotation of microparticles.[13] To generate a fan-shaped beam with OAM, we should tailor a spiral vortex beam to form the fan blade. Thus, a spiral vortex beam with precise control of the spiral angle and beam size should be generated first by phase modulation. Generally, the helical phase of a canonical vortex beam can be expressed as $\exp(il\theta)$, where l is the azimuthal index, (topological charge) which can be either an integer or a fractional number,[16] and θ is the azimuthal angle. In our design, we use an analogous helical phase function $\exp(i\psi)$ to form noncanonical vortex beams[35] (or more precisely asymmetric spiral beams), where ψ is expressed as

$$\psi = 4\pi m_2 \left(\frac{\theta}{2\pi}\right)^2 + m_1 m_2 \theta, \tag{1}$$

where m_1 and m_2 are the two real parameters that control the size and angle of the spiral intensity pattern and θ changes from 0 to 2π. The first term of Eq. (1) $4\pi m_2 \left(\frac{\theta}{2\pi}\right)^2 = 2\pi(2m_2)\left(\frac{\theta}{2\pi}\right)^2$ is the phase equation of power-exponent-phase vortex,[33,34] and the corresponding topological charge is $l = 2m_2$. For the second term of the phase function $m_1 m_2 \theta$, we can get the topological charge is $l = m_1 m_2$. Thus, the total equivalent topological charge from Eq. (1) is

$$l = 2m_2 + m_1 m_2. \tag{2}$$

Typical theoretical and experimental results of the spiral vortex beams are presented in Fig. 1, where the phase distributions [see

Figs. 1(a1)–1(a4)] are constructed by the phase function (1), and the corresponding theoretical and experimental intensity distributions of constructed spiral vortex beams are shown in Figs. 1(b1)–1(b4) and Figs. 1(c1)–1(c4), respectively. Obviously, the variation of the phase gradient in the phase distributions shown in Figs. 1(a1)–1(a4) can be controlled by adjusting the two parameters m_1 and m_2 in Eq. (1). If we just alter the value of m_1 or m_2 in Eq. (1), the phase gradient along the spiral will change correspondingly. As a result, the size and spiral angle of the intensity patterns can be precisely controlled. In the top panels of Fig. 1, from left to right, the parameter $m_1 = 1.6$ is fixed, but the parameter m_2 is changed: $m_2 = 3.5, 7, 10.5$, and 14. The angle of the spiral intensity patterns can be loosely expressed as the length of the white dashed line in Figs. 1(c1)–1(c4). Clearly, as m_2 increases, the size and angle of the spiral intensity pattern also increase. It indicates that parameter m_2 not only can control the size of the spiral intensity pattern but also can modulate the spiral angle. The experimental results in Figs. 1(c) agree well with the simulation results shown in Figs. 1(b). On the other hand, we observe that the radius of the output intensity distributions of the spiral vortex beams is proportional to m_1, whereas the spiral angle does not change remarkably with m_1. Therefore, we can control output intensity patterns of the spiral vortex beams by adjusting the two parameters as needed.

The results above illustrate that we can control the intensity pattern of a single spiral beam at ease. Now, our motivation is to use such spiral beams for the construction of a new type of FOVB that can be applied in optical manipulation in the fluid environment of high particle concentrations.

The experimental setup for creation of various spatial intensity profiles of the FOVB is very similar to that used in our previous work.[36] Essentially, our phase synthesis method (how to "cut" and "paste" the spirals) relies on the "cake-cutting and assembly" approach to achieve the phase gradient for beam shaping. The phase design and corresponding experimental results are presented in Fig. 2, where the first row shows the phase distributions of designed vortex beams under different settings [Figs. 2(a)–2(c)]. The second row [Figs. 2(d)–2(f)] shows the corresponding experimental results of the output intensity distributions. After a series of numerical tests, we found that the phase map [see Fig. 2(a)] with parameters $m_1 = 0.2$ and $m_2 = 32$ is optimal for generation of a large-angle spiral vortex beam [see Fig. 2(d)], and at this time, from Eq. (2), the topological charge $l = 70.4$. Such a vortex beam can be used for generating one of three desired intensity blades for the FOVB [see the dashed white rectangle in Fig. 2(e)]. To assemble the phase for the fan beam, one region [labeled 1 in Fig. 2(a)] was "cut" and "pasted" three times [labeled 2 in Fig. 2(b)] to get the phase distribution in Fig. 2(b). Furthermore, the phase distribution of Fig. 2(c) is the same as Fig. 2(b), except that the area within the dashed black circle was replaced with a uniform phase. By overlapping this uniform phase distribution with a simple blazed grating for the area inside the white dashed circle, the field and corresponding intensity can be filtered out [Fig. 2(c)]. As such, the uniform phase distribution between the dashed black circle and the dashed white circle leads to a donut-shaped "hollow" optical beam in the center of the fan beam, acting as the fan head [Fig. 2(f)].

Next, by employing the above specially tailored FOVB, we experimentally demonstrate optical clearing, optical shielding, and optical transporting of polystyrene beads in colloidal suspensions.
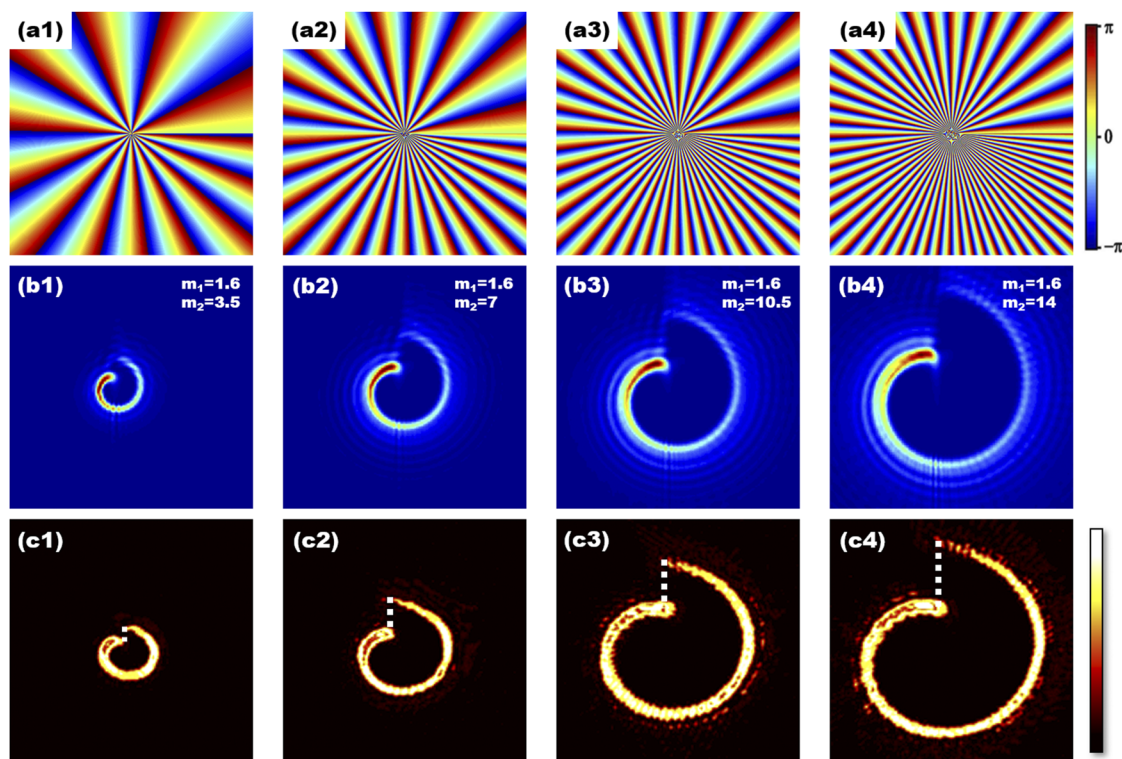
FIG. 1. Numerical and experimental results of proposed spiral vortex beams. (a) Phase distributions of the designed vortex beams by changing parameter m_2 while keeping m_1 fixed. Corresponding numerical (b) and experimental (c) transverse intensity patterns of the output beams. From left to right, $m_1 = 1.6$, and $m_2 = 3.5, 7, 10.5, 14$.

The beads have a 2 μm average diameter, suspended in water. Figure 3 (multimedia view) shows the experimental demonstration of the optical clearing of a target area indicated by the dashed red circle. Figures 3(a1)–3(a4) show the snapshots taken from the corresponding video recorded when the time-lapse is 0 to 17, 36, and 64 s, respectively. When the three-blade FOVB rotates clockwise [see lower inset in Fig. 3(a1)], four microparticles in the circled area are gradually "blown" away as shown in Fig. 3(a) (multimedia view). This is due to the combined action of optical forces (arising from the intensity gradient[37]) and the OAM of the vortex (rising from the phase gradient): the beads covered by the fan got attracted first to the high intensity regions due to gradient forces and then "fanned away" due to the angular momentum from the vortex phase gradient. (We note that the main objective of this paper is to show our beam design and its feasibility for particle clearing, leaving detailed force analysis associated with fan-beam based optical tweezers for future work.) Any impurity in the target area can be rapidly cleared out within about 30 s. As such, the FOVB is used for effective optical clearing— the spiraling of the fan blades is used to "blow" polystyrene particles away from the target area, keeping the area "clean" for a long time.

In some experiments, a target particle is always surrounded by other impurity particles as shown in Fig. 3(b1), which hinders us from trapping the target particle effectively. Especially, due to the Brownian motion, the target is always strongly impacted by

the surrounding particles in a fluid environment of high particle concentrations. In order to solve this problem, using the modified fan beam as shown in Fig. 2(f) that can solely trap the target particle is highly essential. As we see in Fig. 3(b), the target particle [pointed by the red arrow in Fig. 3(b)] is trapped by the hollow beam [see lower inset of Fig. 3(b1)] in the center of the FOVB. Other particles in the same area would be "blown" away by the clockwise rotated optical spiral beam. It should be noted that when the target particle is trapped by the hollow beam in the center of the fan-shaped beam, the blades of the FOVB cannot affect the trapped particle [see Fig. 3(b3)]. On the other hand, the surrounding particles will be driven and blown away by the blades. As explained earlier, this is due to the combined action of gradient forces and angular momentum from the blades.[21,37] As such, the target particle was separated within 3 s and completely isolated within 14 s as shown in Figs. 3(b1)–3(b3). Therefore, by using a "headed" fan-shaped beam, effective optical trapping and shielding of a target particle through a highly disturbing environment can be effectively carried out [shown in Fig. 3(b)] (multimedia view). We point out that the particle (nearly transparent at the wavelength used) is trapped by the gradient force rather than by the absorption-based photophoretic force as done previously with optical bottle beams.[30] Here, to have the right beam size for the fan head and to reduce the scattering force for the trapped particle, the hollow beam is used *in lieu* of a bright Gaussian beam. As seen clearly in Fig. 3(b3), the target particle is trapped by the
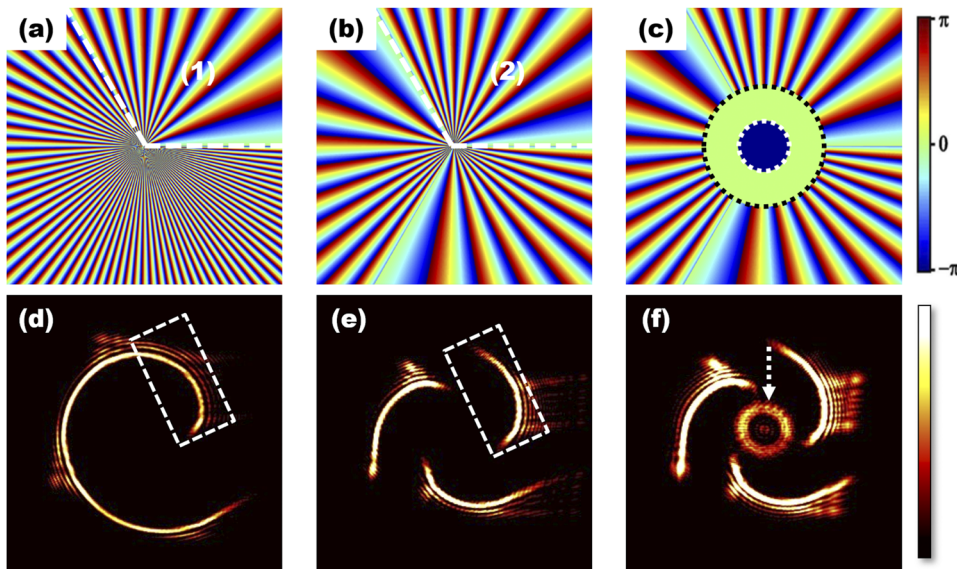
FIG. 2. Experimental demonstration of FOVB by phase assembly of the spiral vortex beams. Top panels: phase patterns. Bottom panels: experimentally observed intensity patterns. (a) The phase distribution of a modulated spiral beam with parameters $m_2 = 32$ and $m_1 = 0.2$, and (d) the corresponding experimental intensity pattern, for which the effective charge of the spiral vortex is $l = 70.4$. [(b) and (e)] Cut-and-paste assembly of the phase from (a) to form the three-blade pattern. [(c) and (f)] Generation of an FOVB by adding a donut-shaped uniform phase pattern in the central area and eliminating the field inside the white dashed circle.

whole hollow beam (which is slightly smaller than the particle) rather than inside the dark core.

Finally, we perform an optical transporting experiment to show that the above rotating FOVB can also be used for optical transportation of a trapped particle to a predefined destination bypassing the obstacles along the way through densely scattering particle suspensions. Figure 4 (multimedia view) shows the experimental demonstrations of optical transporting of the particle by such FOVB. For the convenience of operation, we use the FOVB to capture the particle and move the sample to observe the phenomenon. The red arrow points the 2 μm target polystyrene microparticle which needs to be transported. The red dashed arrow shows the moving direction

and path of the trapped particle, and the areas marked by the dashed red circle in Fig. 4 are the destination of the target. As shown in Figs. 4(a)–4(e), when there are obstacles in the moving direction of the target particle which has been captured by the central hollow optical beam, the impurities will be "blown" away by the rotated FOVB. Thus, the trapped particle can ignore the obstacle particles on the moving path [see clearly in corresponding video file of Fig. 4 (multimedia view)]. As a result, the target particle can be transported along a straight path (or any curved path) to the destination although impurities and perturbations are present in its surrounding environment. Therefore, we have proved that this rotating FOVB can be applied in optical clearing and transporting a trapped
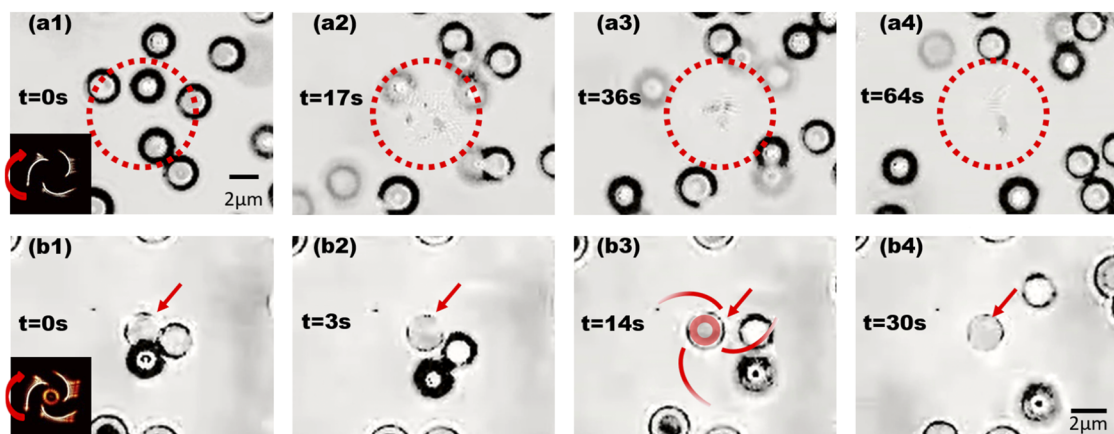

FIG. 3. Experimental demonstration of optical clearing and shielding of a particle (2 μm polystyrene bead) by the FOVB [shown in lower insets in (a) and (b)]. (a) The optical cleared area is marked by a dashed red circle. (b) The target microparticle (marked by a red arrow) is trapped in the center of the fan beam, while others are "blown" away. A simple schematic diagram for the intensity distribution of the FOVB is added in Fig. 3(b3). These images are snapshots taken from the corresponding video files. Multimedia views: (a) https://doi.org/10.1063/1.5133100.1 and (b) https://doi.org/10.1063/1.5133100.2
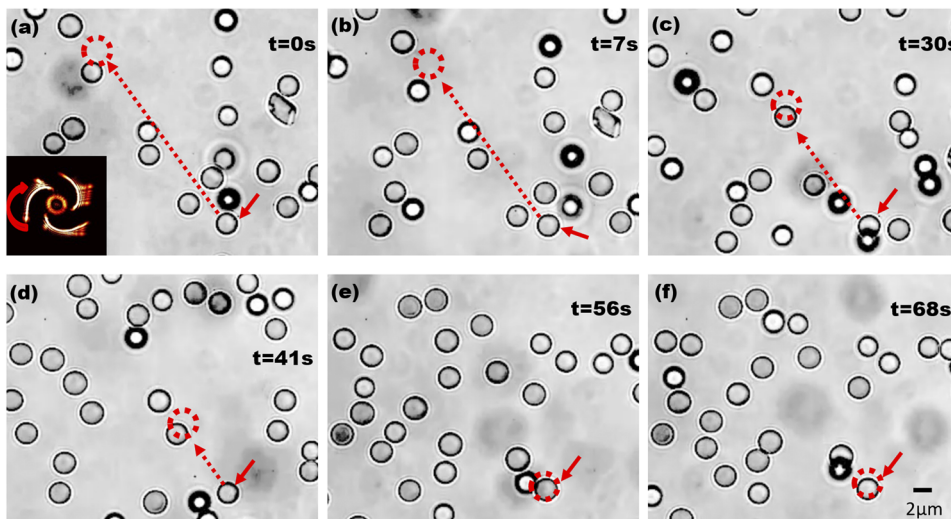
FIG. 4. Experimental demonstration of optical transportation of a target particle (2 μm polystyrene bead marked by a red arrow) by the FOVB. The dashed red arrow shows the direction and the position of the transporting particle, and the dashed red circle marks the destination. For the convenience of operation, we use the fixed FOVB to capture the particle and move the sample cell to observe the phenomenon. (a)-(f) show how the FOVB clears the obstacles and transports the target to the destination, which are the snapshots at the time t = 0s, 7s, 30s, 41s, 56s, 68s, respectively. These images are snapshots taken from the corresponding video files. Multimedia view: https://doi.org/10.1063/1.5133100.3

particle against ambient perturbation. It is worth mentioning that if we change both the rotating direction and the direction of the phase gradient (the topological charges from l to $-l$), the optical fan can attract (rather than repel) the suspended microparticles in the liquid. This may lead to future studies for concentration and guiding particles through a narrow jet flow, which may find applications in microfluidic manipulation, pharmaceutical research, and biology.

III. CONCLUSION

In summary, we have proposed and experimentally demonstrated a new type of spiral optical vortex beam, especially a tailored FOVB with three blade intensity patterns. We have shown that such beams can be used for effective optical clearing and optical shielding and transporting a target particle against impurity contamination even in a crowded environment of high particle concentration. The protection mechanism from our specially designed phase gradient in the fan-shaped vortex beams makes it possible to be applied as an effective shielding and transporting tool for target cells/particles. For instance, the optical microcleaning function of the tailored FOVBs may be quite helpful for quickly separating and sorting different kinds of particles/cells or for large-scale transportation of particles in microfluidic chip[38] or a sick cell from biological environment. Thus, we envisage this research may be applied in biomedical analysis and other fields. Clearly, our work may find applications in optical trapping and manipulation and particularly for microfluidic and biological applications that involve complex environment of the living bodies.[24,39–41]

ACKNOWLEDGMENTS

REFERENCES

[1] A. Ashkin, Phys. Rev. Lett. **24**, 156 (1970).
[2] A. Ashkin and J. M. Dziedzic, Science **235**, 1517 (1987).
[3] F. Kilchherr, C. Wachauf, B. Pelz, M. Rief, M. Zacharias, and H. Dietz, Science **353**, aaf5508 (2016).
[4] T. T. M. Ngo, Q. Zhang, R. Zhou, J. G. Yodh, and T. Ha, Cell **160**, 1135 (2015).
[5] G. D. M. Jeffries, J. S. Edgar, Y. Zhao, J. P. Shelby, C. Fong, and D. T. Chiu, Nano Lett. **7**, 415 (2007).
[6] H. M. Nussenzveig, Eur. Biophys. J. **47**, 499 (2018).
[7] M. Endres, H. Bernien, A. Keesling, H. Levine, E. R. Anschuetz, A. Krajenbrink, C. Senko, V. Vuletic, M. Greiner, and M. D. Lukin, Science **354**, 1024 (2016).
[8] D. Barredo, S. de Leseleuc, V. Lienhard, T. Lahaye, and A. Browaeys, Science **354**, 1021 (2016).
[9] D. Barredo, V. Lienhard, S. De Leseleuc, T. Lahaye, and A. Browaeys, Nature **561**, 79 (2018).
[10] M. L. Juan, M. Righini, and R. Quidant, Nat. Photonics **5**, 349 (2011).
[11] A. N. Grigorenko, N. W. Roberts, M. R. Dickinson, and Y. Zhang, Nat. Photonics **2**, 365 (2008).
[12] O. M. Marago, P. H. Jones, P. G. Gucciardi, G. Volpe, and A. C. Ferrari, Nat. Nanotechnol. **8**, 807 (2013).
[13] H. He, M. E. J. Friese, N. R. Heckenberg, and H. Rubinsztein-Dunlop, Phys. Rev. Lett. **75**, 826 (1995).
[14] J. E. Curtis and D. G. Grier, Phys. Rev. Lett. **90**, 133901 (2003).
[15] C. H. J. Schmitz, K. Uhrig, J. P. Spatz, and J. E. Curtis, Opt. Express **14**, 6604 (2006).
[16] S. H. Tao, X. C. Yuan, J. Lin, X. Peng, and H. B. Niu, Opt. Express **13**, 7726 (2005).
[17] J. Zhao, I. D. Chremmos, D. Song, D. N. Christodoulides, N. K. Efremidis, and Z. Chen, Sci. Rep. **5**, 12086 (2015).
[18] Y. Liang, M. Lei, S. Yan, M. Li, Y. Cai, Z. Wang, X. Yu, and B. Yao, Appl. Opt. **57**, 79 (2018).
[19] A. A. Kovalev, V. V. Kotlyar, and A. P. Porfirev, Opt. Lett. **41**, 2426 (2016).
[20] B. Hadad, S. Froim, H. Nagar, T. Admon, Y. Eliezer, Y. Roichman, and A. Bahabad, Optica **5**, 551 (2018).
[21] M. Padgett and R. Bowman, Nat. Photonics **5**, 343 (2011).
[22] D. G. Grier, Nature **424**, 810 (2003).
[23] K. Dholakia and T. Cizmar, Nat. Photonics **5**, 335 (2011).
[24] X. Wang, S. Chen, M. Kong, Z. Wang, K. D. Costa, R. A. Li, and D. Sun, Lab Chip **11**, 3656 (2011).

[25] G. Xu, K. S. Wilson, R. J. Okamoto, J.-Y. Shao, S. K. D1utcher, and P. V. Bayly, Biophys. J. **110**, 2759 (2016).

[26] K. Lee, A. V. Danilina, M. Kinnunen, A. V. Priezzhev, and I. Meglinski, IEEE J. Sel. Top. Quantum Electron. **22**, 365 (2016).

[27] J. Baumgartl, M. Mazilu, and K. Dholakia, Nat. Photonics **2**, 675 (2008).

[28] J. Baumgartl, T. Cizmar, M. Mazilu, V. C. Chan, A. E. Carruthers, B. A. Capron, W. McNeely, E. M. Wright, and K. Dholakia, Opt. Express **18**, 17130 (2010).

[29] M. P. Lee, A. Curran, G. M. Gibson, M. Tassieri, N. R. Heckenberg, and M. J. Padgett, Opt. Express **20**, 12127 (2012).

[30] P. Zhang, Z. Zhang, J. Prakash, S. Huang, D. Hernandez, M. Salazar, D. N. Christodoulides, and Z. G. Chen, Opt. Lett. **36**, 1491 (2011).

[31] A. G. Banerjee, S. Chowdhury, W. Losert, and S. K. Gupta, IEEE Trans. Autom. Sci. Eng. **9**, 669 (2012).

[32] A. G. Banerjee, A. Pomerance, W. Losert, and S. K. Gupta, IEEE Trans. Autom. Sci. Eng. **7**, 218 (2010).

[33] P. Li, S. Liu, T. Peng, G. Xie, X. Gan, and J. Zhao, Opt. Express **22**, 7598 (2014).

[34] G. Lao, Z. Zhang, and D. Zhao, Opt. Express **24**, 18082 (2016).

[35] G. Molina-Terriza, E. M. Wright, and L. Torner, Opt. Lett. **26**, 163 (2001).

[36] H. P. Wang, L. Q. Tang, J. N. Ma, X. Y. Zheng, D. H. Song, Y. Hu, Y. G. Li, and Z. G. Chen, Photonics Res. **7**, 1101 (2019).

[37] Y. Roichman, B. Sun, Y. Roichman, J. Amato-Grill, and D. G. Grier, Phys. Rev. Lett. **100**, 013602 (2008).

[38] W. Zhan, M. J. Yang, and W. Z. Song, Appl. Phys. Express **12**, 122004 (2019).

[39] D. Gao, W. Ding, M. Nieto-Vesperinas, X. Ding, M. Rahman, T. Zhang, C. Lim, and C.-W. Qiu, Light: Sci. Appl. **6**, e17039 (2017).

[40] M.-C. Zhong, X.-B. Wei, J.-H. Zhou, Z.-Q. Wang, and Y.-M. Li, Nat. Commun. **4**, 1768 (2013).

[41] P. L. Johansen, F. Fenaroli, L. Evensen, G. Griffiths, and G. Koster, Nat. Commun. **7**, 10974 (2016).